We are IntechOpen,
the world's leading publisher of
Open Access books
Built by scientists, for scientists

6,900
Open access books available

185,000
International authors and editors

200M
Downloads

Our authors are among the

154
Countries delivered to

TOP 1%
most cited scientists

12.2%
Contributors from top 500 universities

CLARIVATE ANALYTICS
BOOK CITATION INDEX
INDEXED

WEB OF SCIENCE™

Selection of our books indexed in the Book Citation Index
in Web of Science™ Core Collection (BKCI)

Interested in publishing with us?
Contact book.department@intechopen.com

Co-deposited Ni-Cr-B Nanocomposite Coatings for Protection Against Corrosion-Erosion

Jorge Morales Hernández,

María de Lourdes Montoya García,

Héctor Javier Dorantes Rosales and

Joel Moreno Palmerin

Additional information is available at the end of the chapter

Abstract

Electrodeposition is a low-cost and low-temperature method for producing metal matrix composite coatings. The electrodeposition of Ni matrix/Ni-Cr-B particles is considered as the co-deposition of Ni-Cr-B particles in a Ni matrix, resulting in nanocomposite coatings that can offer good wear and corrosion resistance between other applications. For comparison, the electrodeposition of Ni films and their wear and corrosion evaluation were also carried out under the same conditions. Some coatings usually contain oxide or carbide particles in micrometer size and are electrodeposited in a nickel matrix; however, the use of the mechanical alloying process offers the possibility to reduce the particle size in the order of nanometers obtaining solid solutions, amorphous phases, or intermetallic compounds during the development of new alloys to be co-deposited, improving the engineering materials properties. This kind of nanocomposite can be used in industrial components with an irregular geometry exposed in aggressive environments such as the energy generation and oil industry.

Keywords: co-deposition, nanocomposite coating, erosion-corrosion resistance

1. Introduction

Surface is responsible for the serviceability of the components and the surface engineering is a multidisciplinary activity dedicated to modify the surface according to their functional necessity and where the substrate do not have the capacity. Surface characteristics for engineering applications and in our daily life are:

- Decorative and esthetic

- Thermal barrier

- Better mechanical properties

- Electronic or electrical properties

- Corrosion resistance

- Wear resistance between others

As indicated by other authors, these properties can be enhanced by microstructural changes and phase transformations (metallurgically), by deformations (mechanically), by chemical reactions, and diffusion that modify the surface chemistry or by adding coatings by physical and chemical methods [1]. Industrial plant efficiency can be affected by corrosion and wear damage in such a way that the economic losses associated with this failure mechanism can be quantified as a percentage of a country's gross domestic product annually. In some cases, the corrosion like a failure mechanism may initiate or precede to the wear failure or vice versa, depending of the medium nature; however, the combined effect of corrosion and wear can reduce the component life drastically.

The use of more alloyed steels to improve the surface hardness and corrosion resistance means to use expensive steels with respect to the carbon or low alloy steels, so that several efforts have been made for the protection against corrosion-erosion but with a low efficiency such as the use of inhibitors and the applications of cathodic or anodic currents.

Use of organic, inorganic or metallic coatings have been a good alternative for corrosion and wear protection where the proper selection depends on the accessibility, component size, environment conditions (composition, concentration, pressure, and temperature), and cost; nevertheless, the wide variety of coatings and process development for a lot of corrosive and wear environments are not enough yet, considering which exist different corrosion forms depending on the mechanism of attack that combined with the types of wear, reducing the possibility of getting the best protection.

Tribocorrosion is the concept that explains the surface degradation mechanism when mechanical wear and chemical/electrochemical processes interact with each other [2]. Many industries show damages associated with the tribocorrosion mechanism such as aeronautic, geothermic energy generation, paper industry, and making steel to name a few. To solve the combined failure mechanisms of corrosion and erosion, different alloy systems deposited with the same process have been studied in monolayers as well as multilayers; in this context, the techniques combination, which can offer a variety of coatings with the enough thickness of corrosion protection, with the homogeneous dispersion of fine particles, high hardness, and lubricant properties, has motivated the development of composite coatings where the electrodeposition techniques can offer metal matrix composite coatings, though the co-deposition of nanoparticles with superior properties at low cost.

2. Development of nanocomposite

2.1. Electrochemical nanocomposite coatings (ENC)

Electrodeposition or electroplating process is defined as the deposition of a coating by electrolysis, depositing a substance on an electrode immersed in an electrolyte by the application of electric current through the electrolyte [1]. Modification of the electroplating process includes the occlusions of metallic or nonmetallic particles dispersed in the bath to obtain a composite coating.

Oxides, carbides, silicides, refractory, metallic, and organic powders such as SiC, SiO_2, Al_2O_3, and TiO_2 have been electrodeposited with pure metals to increase strength, harness, wear, and corrosion resistance at the surface with a particle size in the order of microns and current density of 20–200 mA/cm^2 with agitation. The incorporation of a homogeneously dispersed second phase in a metal matrix offers new engineering properties. During the co-deposition, small metal particles added to the plating bath are deposited or embedded simultaneously into a metallic matrix during the electrolytic process [3]. The properties of the composite coating depend on the nature, distribution, and size of the particles in combination with the metallic matrix. The development of a lot of alloying systems by powder metallurgy offers to the composite coating technology, the alternative to increase the opportunities in the solutions of corrosion and wear failures.

Commercial electrolytic baths such as nickel, chromium, copper, and zinc are the metallic matrix, and the dispersed phase is an insoluble solid with nanometric particle size and known morphology, which remains on the cathode surface by agitation and overgrown with the metal electrodeposition [4]. Since the 1970s, the electrodeposited composite coatings have been improved and have been published in some theoretical models that describe the adsorption and electrophoretic migration of particles, until the incorporation of a corrective factor to account for the effects of adsorption and hydrodynamic conditions [5].

Figure 1 reported by Low et al. shows the general process of the co-deposition of particles into decoating, which include: (i) formation of ionic clouds around the particles, (ii) convective movement toward the cathode (convection layer), (iii) concentration boundary layer (diffusion layer), (iv) electrical double layer followed by (v) adsorption and encapsulated of particles. Some theories consider only the transport of particles due to electrophoresis, mechanical entrapment, adsorption, and convective diffusion [5].

Additional to the typical process variables in electroplating such as bath constituents, temperature, pH, current density, agitation, and surfactants is necessary to consider the variables that toward the name of electrochemical co-deposition to obtain composite coatings; these parameters are concentration, size, type, and shape of the particles between others.

Microstructure of the particles can modify the kinetic in such a way γ-Al_2O_3 deposition with copper requests less particle concentration than α-Al_2O_3 [6]. The influence of the particle size and shape are associated with the surface relation, affecting the adsorption of the particles on the cathode, the adsorption of ions on the particle surface, and the suspension stability
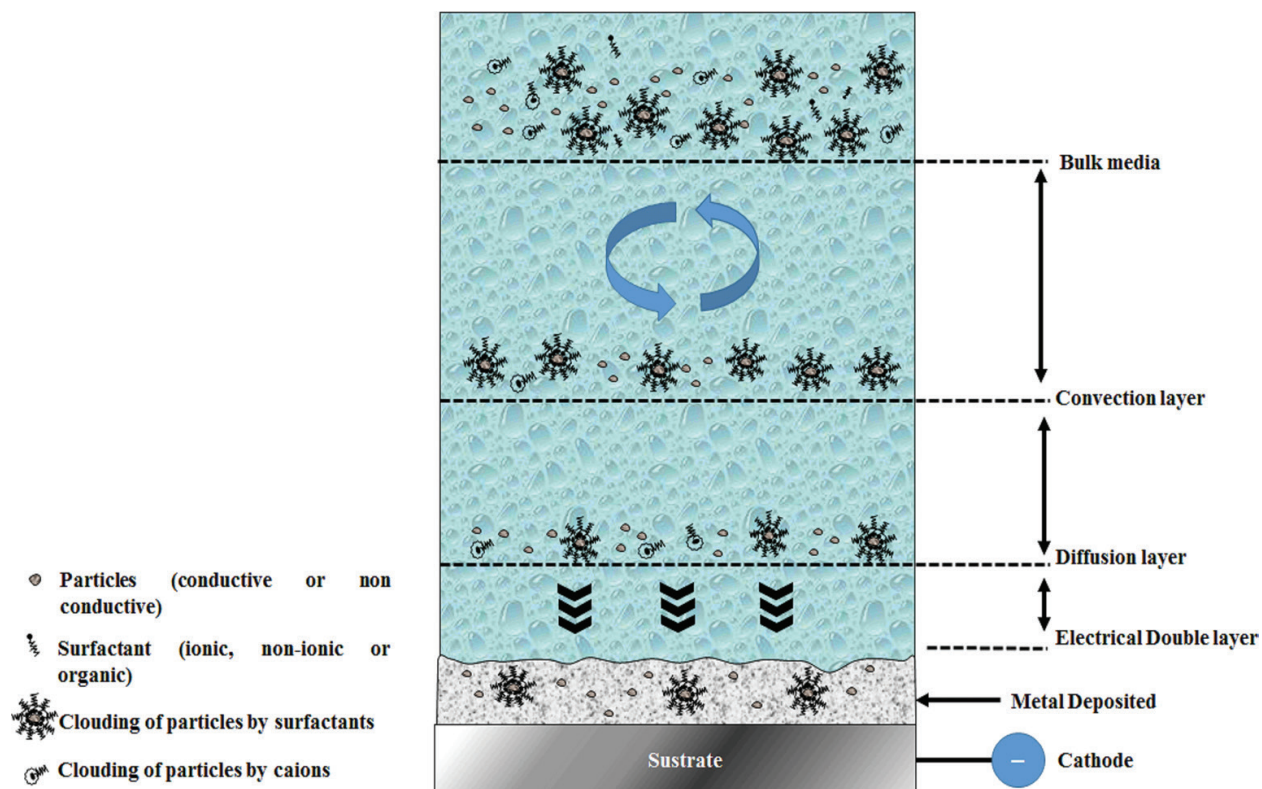
Figure 1. Process involved in the co-deposition of particles into metallic coating [5].

during the co-deposition process. Temperature have a great influence in each co-deposition systems, for example, Ni-Al$_2$O$_3$ is not affected by the temperature on the percentage of embedded particles; on the other hand, the density of particles in the system Ni-Cr increased with the temperature up to 50°C [7].

2.2. Nickel matrix nanocomposite

Nickel matrices electrochemical nanocomposite coatings are characterized by the high hardness, corrosion–erosion resistance, and good appearance and which depends on the dispersed particles whose affinity with nickel could be correlated with their position in the electromotive force series (emf).

Diamond particles with a spherical shape and a concentration of 30 g/L in the bath were electrodeposited in a nickel matrix. Differences in the diamond to nondiamond ratio of carbon forms modified the adsorption characteristics and the quantity of diamond particles in coating (0.2–1 wt%). Largest density of particles into the nickel coating was achieved with the minimum diamond to nondiamond ratio, improving wear resistance and microhardness from 250 to 440 kg/m^2 with respect to pure nickel coating [4]. Hard materials like WC and SiC in a nickel matrix are used in engine block of aluminum alloys with good results in abrasion protection.

The expansion of the electrochemistry of composite materials to new areas includes application in electrocatalysis where hydrophobic Ni + PTFE composite electrodes for electrochemical reactions of water soluble organic substrates reported the evolution of oxygen and hydrogen

at a lower overpotential on Ni + PTFE than on pure Ni. Combinations with $LaNiO_3$, RuO_2, metallic powders, TiO_2, and FeS reported that the most efficiency in catalysis was observed with the Ni + RuO_2 composite. The development of composites for photoelectrocatalysis applications consists of an electrochromic matrix and a semiconducting dispersed phase. In this case, the semiconductor particles are optically excited and electrons are transferred from the conduction band to the electrochromic material, which change color because of redox reaction. Secondary lithium batteries have been investigated with polypyrrole (Ppy) matrix with high concentration of MnO_2 particles [6].

Composite coatings for dry self-lubricating surfaces in automotive and industrial applications were studied by the co-deposition of graphite and MoS_2 nanoparticles in a nickel matrix, obtaining a low friction coefficient of 0.5 and with the double the wear resistance with respect to the steel substrate. CrAlY powder in cobalt or nickel matrix have been co-deposited with better results with respect to the same coating deposited with plasma sprayed because of less porosity. Aluminum particles co-deposited in a nickel matrix and heat treatment reported a nickel–aluminum intermetallic coating with excellent oxidation resistance [1].

2.3. Nanomaterials by mechanical alloying

Scientists and engineers have developed alternative processes to synthesize new materials that by the conventional methods are expensive or complicate. Rapid solidification process (RSP) and mechanical alloying (MA) are two such processing methods to produce equilibrium and metastable phases. MA was implemented to produce oxide dispersion strengthened (ODS) nickel and iron based superalloys for applications in the aerospace industry in 1966 [8].

MA is a dry powder processing technique involving cold welding, fracturing, and rewelding between clean surfaces in contact with elemental or combined powders exposed to high-energy collision in a high-energy ball mill. Development by Benjamin to produce an oxide dispersion-strengthening alloy with γ' precipitation hardening in nickel-based superalloys intended for gas turbine applications. The alloying of immiscible elements is possible by MA, increasing the solubility limit with respect to the equilibrium diagrams.

Elemental powders mixture is loading with grinding medium (ceramic or hardened steel) in a stainless-steel container sealed after be exposed at vacuum cycle and under inert atmosphere to avoid reaction with the ambient. Usually, 1–2 wt% of a process control agent (stearic acid or alcohol) is normally added to maintain an equilibrium between the welding and fracture events, especially when ductile–ductile mixture is milled. The high-energy mills are SPEX mill (10 g of powder), attritors (few pounds of powder), or planetary mills with two or more containers can be processed at a time. Since, the 1980s have been synthesized many alloy phases including equilibrium and supersaturated solid solutions, crystalline and quasicrystalline intermediate phases, and amorphous or glassy alloys [8]. Reduction of grain size of few nanometers (<100 nm) of powder mixtures by MA introduced the concept of nanocrystalline materials before the concept of nanotechnology. The research, technology development, and innovations in MA have applications in different industrial requests as is shown in **Figure 2**.
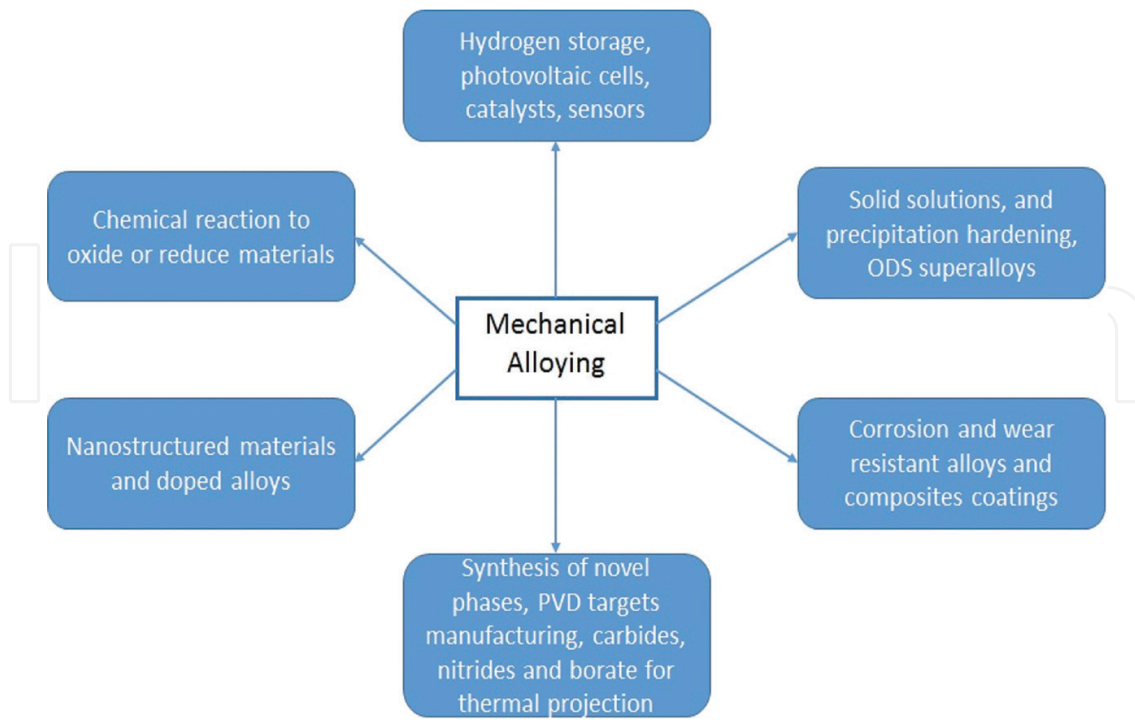
Figure 2. Potential applications of mechanically alloyed products [8].

During the particles reduction by fracturing and rewelding of the powders, the reaction area increases and the diffusion distance between particles is minimized with the introduction of many crystal defects as a function of the time during MA [9]. Thermal energy of the particles produce that all the atoms vibrate about their equilibrium position, resulting in a jump of an interstitial atom to an adjacent interstice after the atoms of the parent lattice must be forced apart into higher energy position. Activation energy for diffusion is equal to the sum of the activation energy to form a vacancy and the activation energy to move the vacancy, written as:

$$\Delta Q = \Delta Q_f + \Delta Q_m \tag{1}$$

where ΔQ_f is the activation energy for creating vacancies and ΔQ_m the activation energy for moving vacancies with the temperature increase that is produced during the collisions between particles until it reaches the diffusion temperature.

Energy stored by the accumulate deformation during MA is associated with the creation of dislocations and grain boundaries in the deformed material, if there is sufficient activation energy by deformation process, interstitial and substitutional atoms can move in crystal lattices from one atomic site to another, promoting the diffusion process. The formation of large number of defects (dislocation and vacancies) generated by thermal energy in conventional process in MA is active by mechanical deformation during the high-energy collision between powder particles, being the activation energy for the diffusion that obey the first law of Gibbs of diffusion written as:

$$D = D_o \exp\left[\frac{-\left(\Delta Q_f + \Delta Q_m\right)}{RT}\right] \tag{2}$$

where D is the diffusion coefficient, D_o is the diffusion coefficient where $T = 0$, R is the universal gas constant, and T is the temperature in Kelvin.

Equation (2) establishes that at the same value of D, a decrease in activation energy is equivalent to an increase in temperature, situation that is present punctually during the particle size reduction and the increase of surface energy where the localized temperature can increase considerably. It is believed that lowering activation energy is present in the MA process [9]. In the melting process, the diffusion is controlled by thermal energy; in mechanical alloying, formation of new alloys is determinate by both thermal and mechanical energies. By creating nanometer crystalline through repeated fracturing and cold welding of powder particles, diffusion take place through the grain boundaries, increasing the solubility limits inclusive in difficult alloying systems.

2.4. Ni-Cr-B nanocomposite coatings

2.4.1. Experimental

Mechanical alloying process was implemented to synthetize nanoparticle with a nominal composition of Ni-20Cr-10B (wt%) from elemental Ni, Cr, and B of 99.95, 99.80, and 99.5% purity, respectively. The powders were loaded in steel vials with hardened balls of 4.76 and 12.7 mm in diameter. The charged vial was evacuated with a vacuum pump for 20 min and then filled with argon gas in a glove box. Ethyl alcohol (1.5 c.c.) was used as the process control agent (PCA) to prevent the agglomeration of powders during milling. The high-energy equipment used was the SPEX mill 800 with a powder to ball weight ratio of 6:1 and a total sample weight of 28 g. The powders were processed until complete 40 h of milling. The phase structure of milled powders was characterized with X-ray diffraction (XRD) using a Bruker D8 advanced diffractometer with Cu Kα radiation ($\lambda = 1.54056$ nm) and operated at 40 kV and 40 mA. Powder morphology and particle size (maximum milling time) were characterized by using a JEOL 2000 scanning electron microscopy (SEM). Validation of particle size was made with a Zeta Sizer equipment model Malvern MPT-2.

Ni-Cr-B powders synthetized by MA and with average particle size of 95 nm in diameter were added in Ni-matrix with the electrochemical deposition process from a nickel sulfate bath containing 270 g/L NiSO$_4$·6H$_2$O, 50 g/L NiCl·6H$_2$O, 35 g/L H$_3$BO$_3$ and 2 g/L of Ni-Cr-B as nanoparticles dispersed under constant magnetic agitation (600 rpm). The pH value of the bath was 4.3 after loading the Ni-Cr-B nanoparticles at constant temperature of 328 K (55°C). Low carbon steel plate with size of 50 mm × 20 mm × 2 mm was used as substrate after abraded it with SiC paper of grades 320, 430, 600, and 1000 and cleaned with ultrasonic in distilled water. Ni plate (99.9% purity) with similar dimensions to the steel was used as a cathode. The current density of 5.8 A/dm^2 was applied during 40 min. For comparison, nickel coating was also deposited with the same parameters and the same bath but without adding of Ni-Cr-B particles.

Surface morphology of the composite was characterized by SEM; cross-sectional was prepared to measure the coating thickness in function of deposition time by optical microscopy. Measurements of the Vickers microhardness were performed on the cross-sectional by using a microhardness tester under a load of 0.45 N for 15 s according to the ASTM E140 standard; the final reported value was the average of 10 measurements.

The friction and wear test were performed at room temperature without lubricant on a ball-on-disc type tribometer with a constant rotation speed of 200 rpm, a constant radius of 2.5 mm and load of 2 N. Hardened steel balls of 10 mm of diameter were used; the test lasted for 1 h for a total distance of 188 m and the value reported was an average of three measurements. After wear test, the worm surfaces were evaluated with optical microscopy.

Corrosion resistance of the coatings was evaluated using the anodic polarization method. The equipment used was a potentiostat/galvanostat BioLogic® with EcLab software. Open circuit potential was monitored until equilibrium was reached and then, the polarization technique was applied with an over potential of ±1 V with a scan rate of 1 mV/s. A typical three electrodes configuration with composite coating as working electrode (WE), platinum mesh as counter electrode (CE), and calomel as reference electrode (RE) were used and immersed in NaCl solution at 3.5 wt% prepared with distilled water [11]. Optical microscopy was used to evaluate the corrosion mechanism in the nickel and composite coatings and their comparison with the corrosion observed at the substrate.

2.4.2. Results and discussion

2.4.2.1. Mechanical alloying of powders

After 40 h of milling, the XRD characterization shows a solid solution (SS) of chromium and boron in nickel matrix (**Figure 3**) with a minimum particle size of 95 nm immersed in an acicular morphology. Initial powder particles of nickel change from angular to acicular powder particles (**Figure 4**) because of the introduction of two dense structures (bcc from Cr and hcp
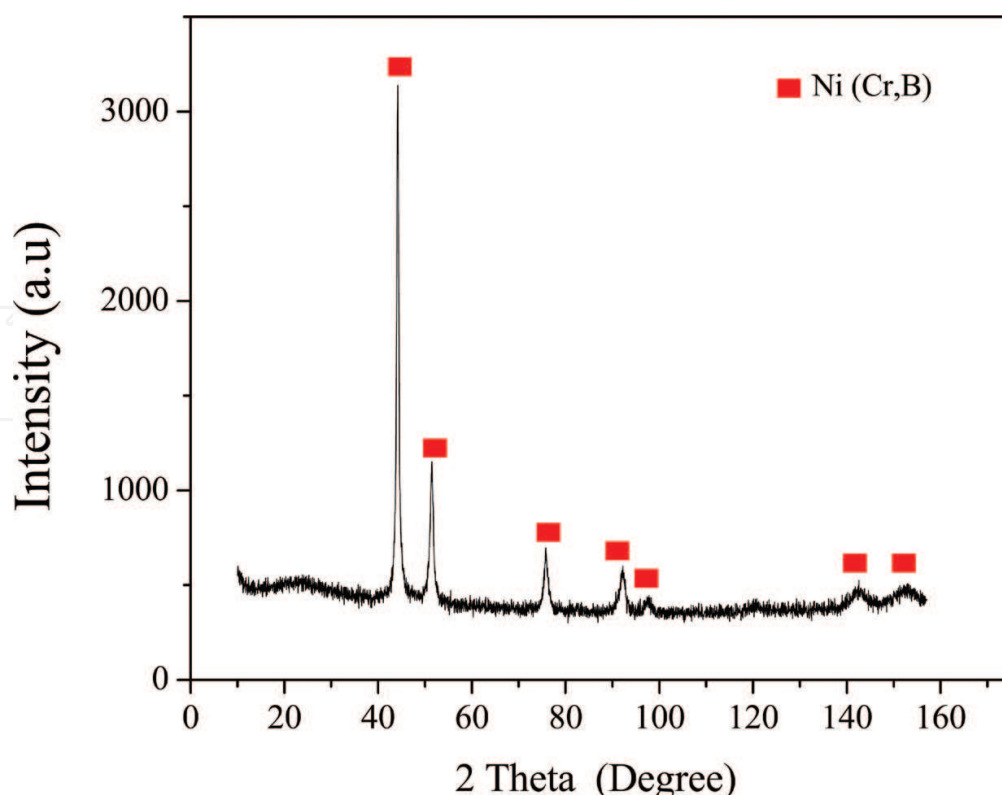
Figure 3. XRD pattern of the mixture Ni-20Cr-10B after 40 h of MA.
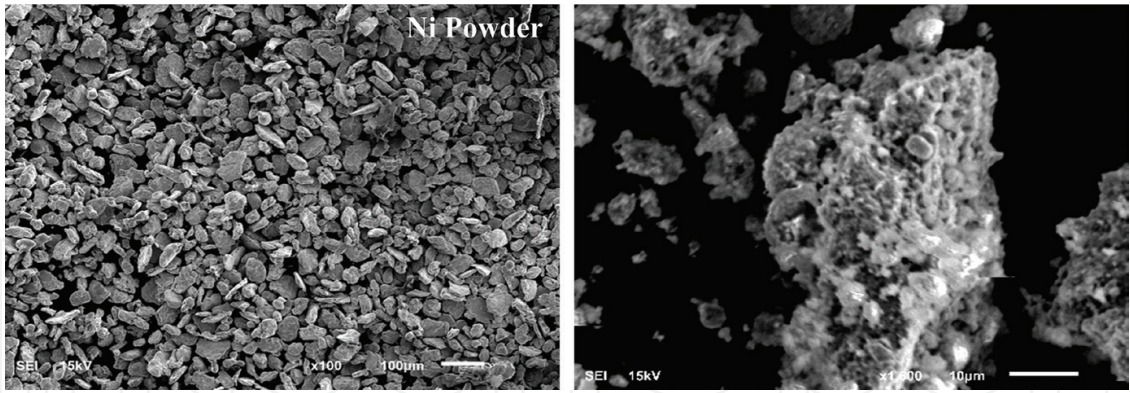
Figure 4. Initial morphology of Ni powders and acicular morphology in the SS after 40 h of milling.

from B) [10]. High ductility of nickel permits that two elements with similar atomic radio can be introduced in their structure. The final powder showed a high reactivity because of the high reduction in particle size and to the high stored energy by deformation.

2.4.2.2. Surface morphology in the coating

Table 1 shows the nickel electroplating thickness and the composite coating thickness at different process time, where the thickness reported was of 13.749 and 22.018 μm to the nickel and composite coatings, respectively at maximum process time. The difference in thickness with or without particles corresponding with the dispersion and over saturation of particles at the coating, resulting in a difference of 8.269 μm in thickness at 2400 s, that can mean the particles deposition without being encapsulated by the Ni matrix. During the first two steps, particles deposition was not detected in the Ni coating.

Figure 5 shows the typical morphology of the nickel electroplating that correspond with a pyramidal morphology and is reported that the surface morphology of the composite coating with 2100 s of deposition, where is observed a homogeneous dispersion of particles that in more proportion are encapsulated in the Ni matrix, identifying some coarse particles deposited over the first encapsulated particles.

When the electrodeposition time is enough, the steeps of boundary layer, electrical double layer, and the encapsulated particles are reduced by the oversaturation of particles that were

Time (s)	Identification code	Thickness (μm)	
		Ni	Ni–Ni-Cr-B
1200	–	7.033	–
1500	–	9.427	–
1800	P1	9.629	14.357
2100	P2	10.365	15.843
2400	P3	13.749	22.018

Table 1. Average thickness of Ni coating and Ni–Ni-Cr-B composite coating vs process time.

transferred in the last two steps (formation of ionic clouds and convective movement) [12]. For these reasons, some particles without being encapsulated are deposited over the first covered particles at the Ni matrix [13]. **Figure 6** shows the composite coating deposited at 2400 s where some conglomerate particles are deposited over the first layer of particles covered by nickel. This second layer shows coarse particles that could be with less adherence at
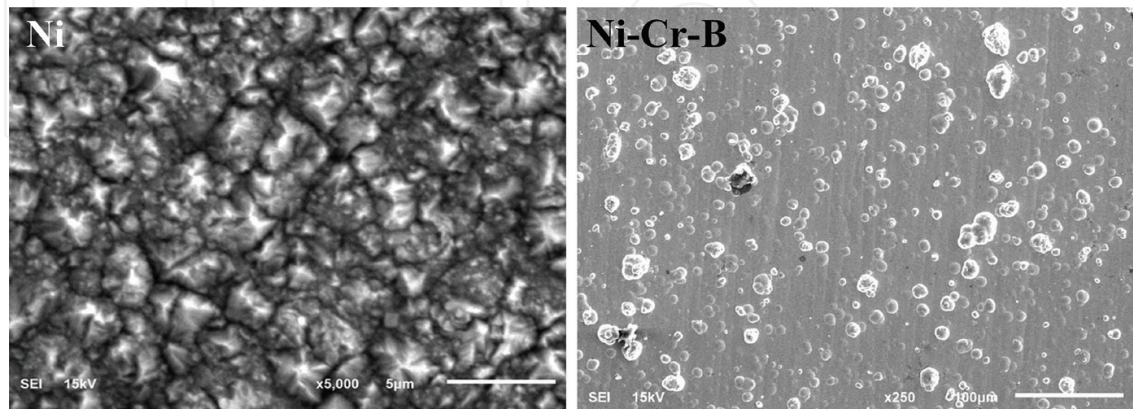
Figure 5. Nickel electroplated surface and Ni–Ni-Cr-B composite coating at 2100 s of process respectively.
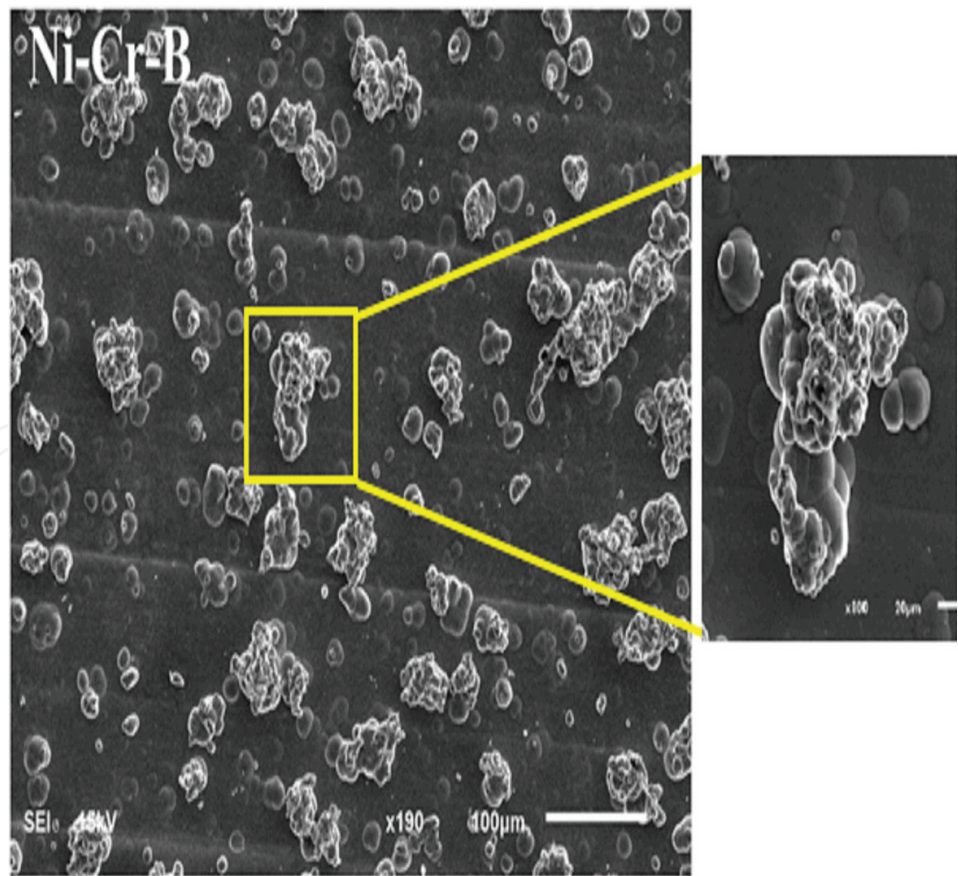
**Figure 6.** Composite coating deposited at 2400 s where some particles are conglomerates.

the substrate and be removed under abrasive wear conditions; however, this situation was not observed.

2.4.2.3. Hardness and wear resistance

Figure 7 shows the hardness from the samples P1, P2, and P3 in comparison with the nickel coating and substrate. Hardness composite coating is approximately 60% upper than the electroplating Ni coating and much more than the substrate. This hardness value is in average similar to obtained by heat treatment in an alloyed steel (59 HRc) for automotive and wear applications.

Friction coefficient from the substrate, Ni coating, and Ni–Ni-Cr-B composites are reported in **Figure 8**. Lubricant condition of the composite coating is observed with the minimum friction coefficient of 0.5 with respect to the Ni plating of 0.64 and carbon steel of 0.72. Differences in the co-deposition time for the composite coatings (samples P1, P2, and P3) do not represent changes in the friction coefficient independently that exist various particles density at the surfaces or in the case where exist an overdeposition of particles or conglomerates at the maximum process time, indicating the friction coefficient reported represents the composite coating nature.

Width of friction marks and appearance shows an adhesive wear condition for the Ni plating and composite coatings [14]; however, less footprint width was observed for the composite
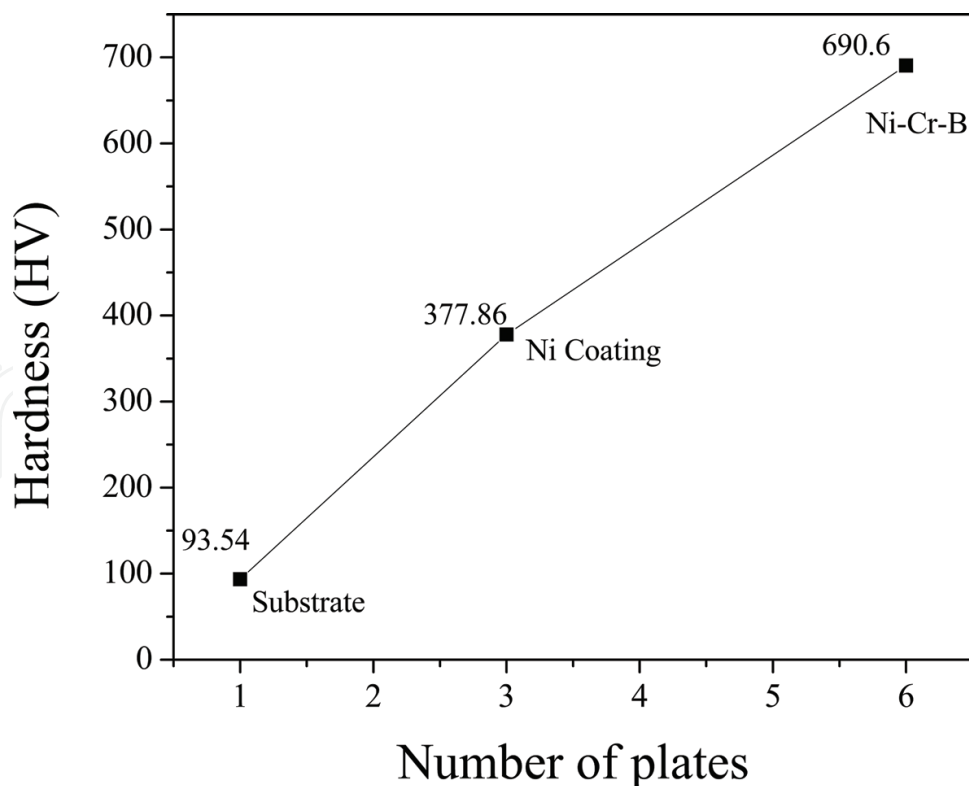

Figure 7. Vickers hardness of the composite coatings from the samples P1, P2, and P3 with respect to the Ni coating and substrate hardness.

coatings as is shown in **Figure 9**. Summarized of tribology properties is shown in **Table 2**, where the lowest friction coefficient and highest hardness reported in the composite coatings, represents a coating that can be used under abrasive operation conditions.
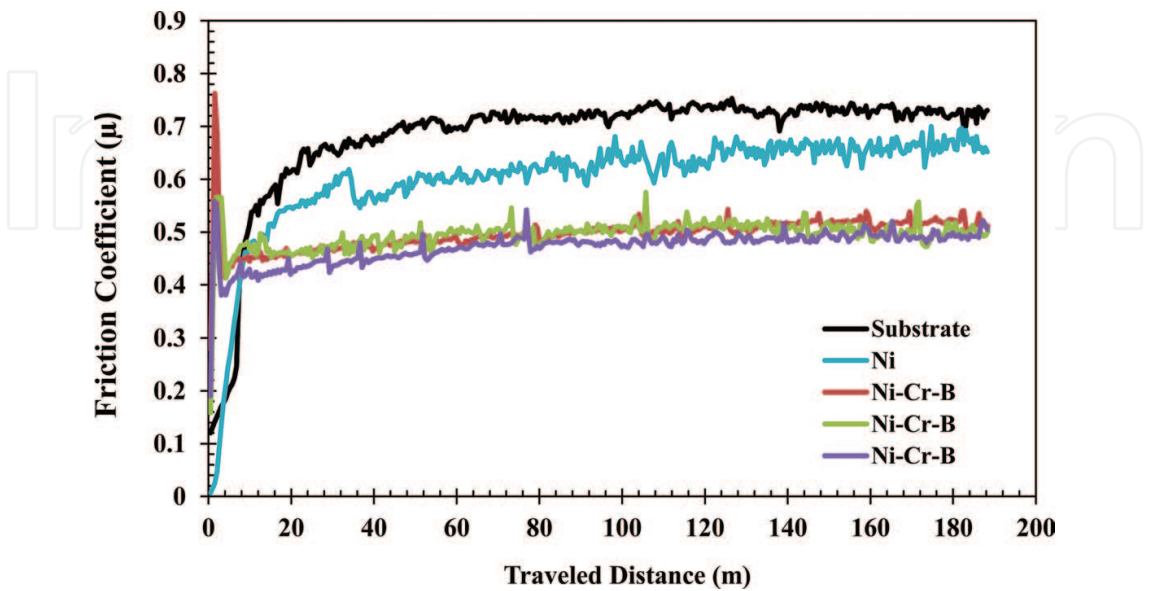
Figure 8. Friction coefficient of carbon steel, pure Ni, and Ni–Ni-Cr-B composite coatings (samples P1, P2, and P3).
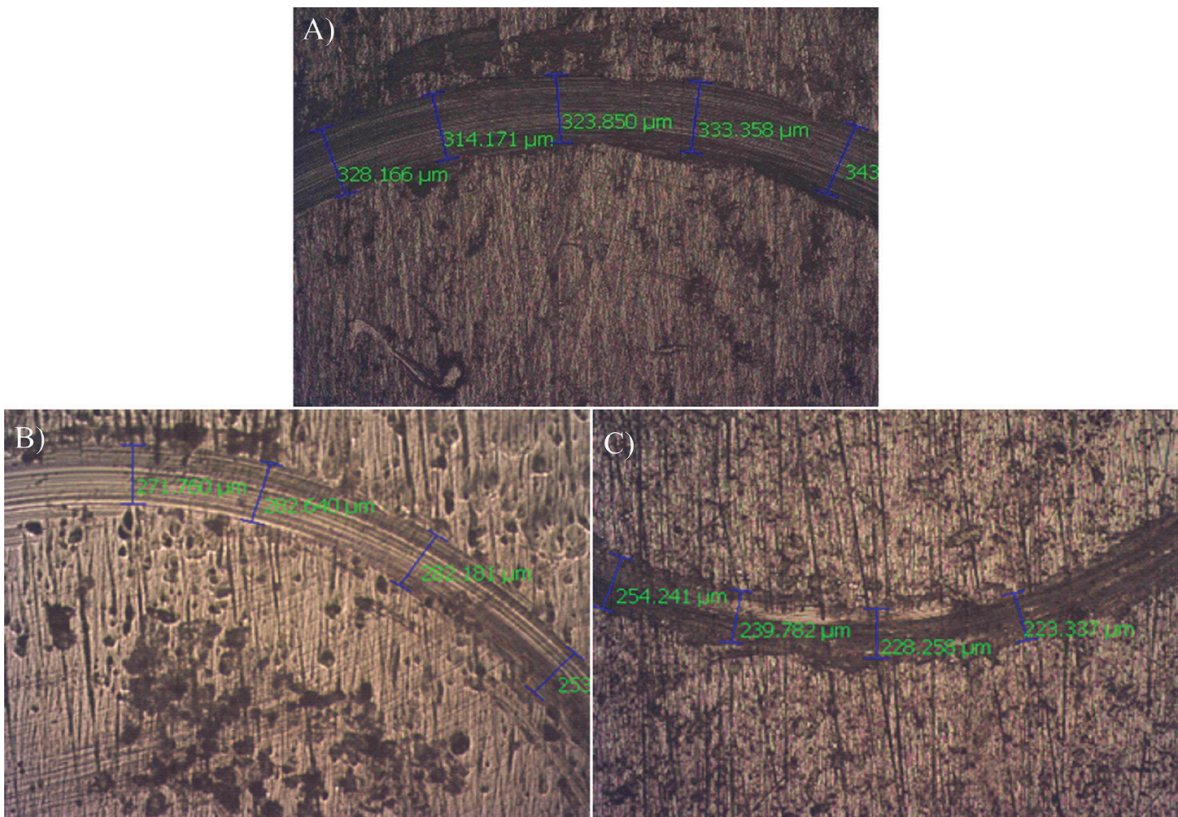
Figure 9. Footprint width for the coatings after evaluating their wear resistance for: (A) carbon steel substrate, (B) Ni plating coatings, and (C) Ni–Ni-Cr-B composite coating.

Sample	Friction coefficient	Footprint (μm)	Hardness (Hv)
Substrate	0.72	506	93.54
Ni coating	0.64	284.47	377.86
Ni–Ni-Cr-B composite	0.50	213.12	690.6

Table 2. Summarize of the physical properties from the composite and Ni coatings.

2.4.2.4. Corrosion resistance

Polarization plots show that the corrosion resistance of the Ni and Ni-Cr-B composites coatings are slightly similar, but with a higher resistive behavior for the composite coating when moving toward less current density as is reported in **Figure 10**. Minimum passive region in the anodic area was observed for ᴮoth coatings. Corrosion resistance in millimeters per year (mmpy) is reported in **Table 3**, where the composite coating reported good corrosion resistance; however,
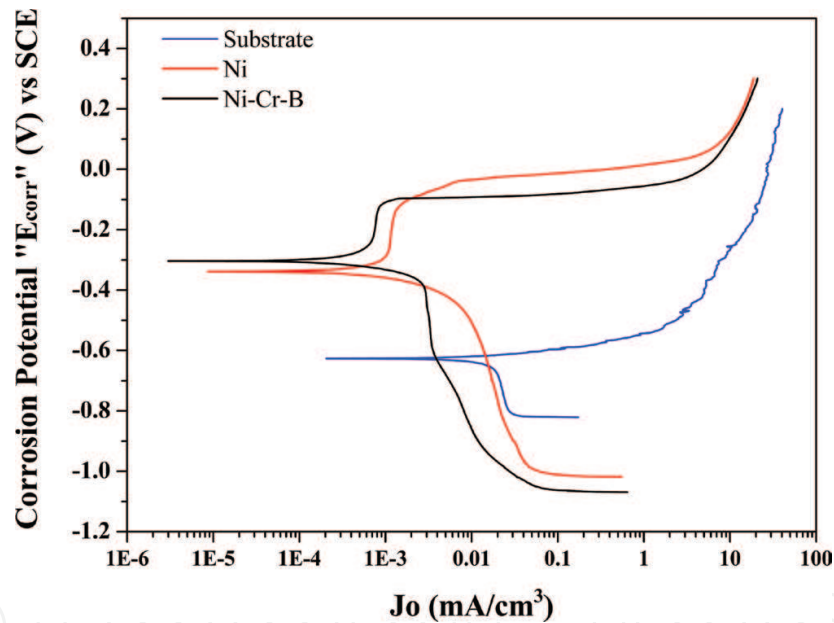
Figure 10. Polarization curves of substrate, Ni plating, and Ni–Ni-Cr-B composite coating, tested in an electrolyte of 3.5 wt% of NaCl.

Sample	V_{corr} (mmpy)
Substrate	2.120
Nickel	0.0093
Ni-Cr-B P1	0.0032
Ni-Cr-B P2	0.0037
Ni-Cr-B P3	0.0037

Table 3. Corrosion resistance in mmpy in the Ni plating and composites coatings.

due to the matrix Ni, the concentration of Ni-Cr-B particles, size, and morphology, not represent a significative difference in the corrosion resistance with respect to nickel coating, being evident the improvement in the abrasión resistance. The general corrosion mechanism observed in the substrate in NaCl was reduced in high magnitude in the nickel matrix composites.

3. Conclusions

Solid solutions of Cr and B in Ni were obtained after 40 h of MA from the elemental powders with a minimum particle size of 95 nm and with an acicular morphology. Due to the high ductility of the mixture and the high deformation energy obtained at the maximum milling time, the nanoparticles were grouped in conglomerates of the order or microns. Different coating thickness were obtained in the Ni plating and composites coatings in function of process time, obtaining a differential in thickness between the Ni pure and Ni-composite in the order of 5.47–8.26 microns and which corresponds with the increase of thickness added by the Ni-Cr-B particles, representing a more dispersion and concentration of particles proportional with the deposition time. High hardness and better wear resistance were obtained in all the composite samples independent of the process time and the particles concentration at the surface, resulting a composite coating with low friction coefficient for lubricant applications and high hardness for wear requirements. Corrosion resistance was improved in the Ni-Cr-B composites coatings lightly with respect to the Ni coating assuming that the composite coating was conformed of a Ni matrix and that the presence and concentration of Ni-Cr-B nanoparticles were not representative to improve the corrosion resistance with respect to Ni coating. We are considering the application of a heat treatment at the composite coating to increase the corrosion resistance.

Acknowledgements

Author details

Jorge Morales Hernández[1]*, María de Lourdes Montoya García[1], Héctor Javier Dorantes Rosales[2] and Joel Moreno Palmerin[3]

*Address all correspondence to: jmorales@cideteq.mx

1 Research Center and Technology Development in Electrochemistry, Querétaro, México

2 School of Chemical Engineering and Extractive Industries, Mexico City, México

3 Autonomous University of Guanajuato, Guanajuato, México

References

[1] J.R. Davis; Surface Engineering for Corrosion and Wear Resistance; ASM International, 2005; pp. 1-159.

[2] R.J.K. Wood; Tribo-corrosion of coatings: A review; Journal of Physics D; 40, 2007; pp. 5502-5521.

[3] J.R. Roos, J.P. Celis, J. Fransaer and C. Buelens; The development of composite plating for advanced materials; Journal of the Minerals, Metals and Materials Society; 42, 11, 1990, pp. 60-63

[4] V.N. Tseluikin; Composite electrochemical coatings: Preparation, structure, properties; Protection of Metals and Physical Chemistry of Surfaces; 45, 3, 2009, pp. 287-301.

[5] C.T.J. Low, R.G.A. Wills, F.C. Walsh; Electrodeposition of composite coatings containing nanoparticles in a metal deposit; Surface & Coatings Technology; 201, 2006, pp. 371-383.

[6] M. Musiani; Electrodeposition of composites: An expanding subject in electrochemical materials science; Electrochemica Acta; 45, 2000, pp. 3397-3402.

[7] A. Hovestad, L.J.J. Janssen; Electrochemical codeposition of inert particles in a metallic matrix; Journal of Applied Electrochemistry; 25, 1995, pp. 519-527.

[8] C. Surynarayana, E. Inavov, V.V. Boldyrev; The science and technology of mechanical alloying; Materials Science and Engineering A; 304-306, 2001, pp. 151-158.

[9] L. Lu and M.O. Lai; Formation of new materials in the solid state by mechanical alloying; Materials & Design; 16, 1, 1995, pp. 33-39.

[10] O.D. Neikov, S.S. Naboychenko, I.V. Murashova, V.G. Gopienko, I.V. Frishberg and D.V. Lotsko, Eds.; Handbook of None-ferrous Metal Powders, Technology and Applications, first edition; Elsevier, 2009.

[11] A. Mandujano Ruiz, J. Morales Hernández, F. Castañeda Saldivar, H. Herrera Hernández and J.M. Juárez García; Determination of the Kinetic Parameters for Stainless Steel 304 Exposed in Chloride Solution from Electrochemical Noise; in review to be published.

[12] S. Srikomol, Y. Boonyongmaneerat and R. Techapiesancharoenkij; Electrochemical code-position and heat treatment of nickel-titanium alloy layers; Metallurgical and Materials Transactions B, 44B, 2013, pp. 53-61.

[13] H.-K. Lee, H.-Y. Lee, J.-M. Jeon; Codeposition of micro and nano-sized SiC particles in the nickel matrix composite coatings obtained by electroplating; Surface and Coatings Technology; 201, 8, 2007, pp. 4711-4717.

[14] Z. Yue-bo, Z. Guo-gang, Z. Hai-jun; Fabrication and wear properties of co-deposited Ni-Cr nanocomposite coatings; Transactions of Nonferrous Metals Society of China; 20, 2000, pp. 104-109.